The effect of hypoxia on gill morphology and ionoregulatory status in the Lake Qinghai scaleless carp, *Gymnocypris przewalskii*

Victoria Matey[1], Jeffrey G. Richards[2], Yuxiang Wang[3], Chris M. Wood[4], Joe Rogers[4], Rhiannon Davies[3], Brent W. Murray[5], X.-Q. Chen[6], Jizeng Du[6,*] and Colin J. Brauner[2,†]

[1]Department of Biology, San Diego State University, San Diego, CA, USA, [2]Department of Zoology, University of British Columbia, Vancouver, BC, V6T 1Z4, Canada [3]Department of Biology, Queen's University, Kingston, Ontario, KZP 3N6, Canada, [4]Department of Biology, McMaster University, Hamilton, Ontario, L8S 4K1, Canada, [5]Ecosystem Science and Management Program, University of Northern British Columbia, Prince George, BC, V2N 4Z9, Canada, [6]Department of Biotechnology, Life Science College, Zhejiang University, Hangzhou, Zhejiang 310027, People's Republic of China

*Author for correspondence in Chinese (e-mail: dujz@zju.edu.cn)
†Author for correspondence (e-mail: brauner@zoology.ubc.ca)

Accepted 30 January 2008

SUMMARY

Goldfish and crucian carp at low temperature exhibit plasticity in gill morphology during exposure to hypoxia to enhance gas exchange. Hypoxia-induced changes in gill morphology and cellular ultrastructure of the high altitude scaleless carp from Lake Qinghai, China, were investigated to determine whether this is a general characteristic of cold water carp species. Fish were exposed to acute hypoxia (0.3 mg O_2 l^{-1}) for 24 h followed by 12 h recovery in normoxic water (6 mg O_2 l^{-1} at 3200 m altitude), with no mortality. Dramatic alterations in gill structure were initiated within 8 h of hypoxia and almost complete by 24 h, and included a gradual reduction of filament epithelial thickness (>50%), elongation of respiratory lamellae, expansion of lamellar respiratory surface area (>60%) and reduction in epithelial water–blood diffusion distance (<50%). An increase in caspase 3 activity in gills occurred following 24 h exposure to hypoxia, indicating possible involvement of apoptosis in gill remodeling. Extensive gill mucous production during hypoxia may have been part of a general stress response or may have played a role in ion exchange and water balance. The large increase in lamellar surface area and reduction in diffusion distance presumably enhances gas transfer during hypoxia (especially in the presence of increased mucous production) but comes with an ionoregulatory cost, as indicated by a 10 and 15% reduction in plasma [Na⁺] and [Cl⁻], respectively, within 12–24 h of hypoxia. Within 12 h of hypoxia exposure, 'wavy-convex'-mitochondria rich cells (MRCs) with large apical crypts and numerous branched microvilli were transformed into small 'shallow-basin' cells with a flattened surface. As the apical membrane of MRCs is the site for active ion uptake from the water, a reduction in apical crypt surface area may have contributed to the progressive reduction in plasma [Na⁺] and [Cl⁻] observed during hypoxia. The changes in the macro- and ultra-structure of fish gills, and plasma [Na⁺] and [Cl⁻] during hypoxia were reversible, showing partial recovery by 12 h following return to normoxia. Although the large morphological changes in the gill observed in the scaleless carp support the hypothesis that gill remodeling during hypoxia is a general characteristic of cold water carp species, the reduced magnitude of the response in scaleless carp relative to goldfish and crucian carp may be a reflection of their more active lifestyle or because they reside in a moderately hypoxic environment at altitude.

Key words: gill morphology, hypoxia, ionoregulation, mitochondria rich cell, osmorespiratory compromise.

INTRODUCTION

The fish gill is a multifunctional organ that is the dominant site for gas exchange, ionoregulation, acid–base balance and nitrogenous waste excretion (Evans et al., 2005). Gill morphology that enhances one of these processes may impair another, and thus gill design represents a compromise among competing demands (Brauner et al., 2004; Sollid and Nilsson, 2006). Recently, there have been a number of studies showing that gill morphology in many teleost fishes is plastic (Sollid et al., 2003; Brauner et al., 2004; Ong et al., 2007) and can be greatly altered within hours to days during exposure to hypoxia (van der Meer et al., 2005; Sollid and Nilsson, 2006). Perhaps one of the most extreme illustrations of this is found in the crucian carp where in normoxia at 8°C the lamellae are almost indiscernible because of a large interlamellar mass. In fish exposed to hypoxia (0.75 mg O_2 l^{-1}), there is a complete remodeling of the gills over the course of several days, which includes gradual transformation of thick filaments with no visible respiratory lamellae, into filaments supporting two rows of well developed lamellae (Sollid et al., 2003; Sollid et al., 2005). Liberation and expansion of respiratory lamellae become possible because of a high rate of apoptosis and low rate of cell proliferation in the filament epithelium that cause a decrease in cell mass and epithelial shrinkage (Sollid et al., 2003). The result is over a sevenfold increase in total gill surface area greatly facilitating oxygen transport, but these changes appear to come at a cost to ion regulation (Sollid et al., 2003). These alterations are completely reversible within days following transfer from hypoxic back to normoxic water (Sollid et al., 2003).

The presence of such a large interlamellar mass in normoxia has been proposed as a mechanism for reducing water and/or ion fluxes across the gills, while still providing a sufficient surface for gas exchange. The reduced diffusion capacity of the gills in normoxia

is partially compensated for by a very high blood oxygen affinity in the crucian carp (Sollid et al., 2005). The goldfish at low temperature also exhibits a large interlamellar mass in normoxia that is greatly reduced in hypoxia. Both crucian carp and goldfish (*Carassius carassius*) are renowned for their hypoxia tolerance, which is at least in part related to their high blood–oxygen affinity (Sollid et al., 2005) and the latter may be a prerequisite for the possession of a low gill surface area in normoxia.

Although gross morphological changes in the gills of carp and goldfish during exposure to hypoxia have been relatively well documented, changes to specialized cells in the gill epithelium during exposure to hypoxia and associated gill remodeling have been largely unexplored but are likely of great significance during acclimation. The complex epithelium of the gill consists primarily of mitochondria-rich cells (MRC), pavement cells (PVC) and mucous cells (MC). Current morphological classification of ion transporting MRCs is based on their surface topography, internal ultrastructure, and location in the filament epithelium (Perry, 1997; Wilson and Laurent, 2002; Evans et al., 2005). Based upon surface structure, there appear to be three types of MRCs in the gill and operculum epithelia (Lee et al., 1996; Chang et al., 2001; Chang et al., 2002; Shieh et al., 2003). These are the 'deep-hole' MRCs with a distinctive apical crypt, formed by a deeply invaginated apical membrane recessed below neighboring cells; the 'shallow-basin' MRCs with a slightly recessed or flat apical surface; and the 'wavy-convex' MRCs which possess a convex apical membrane with wavy microvilli extending above neighboring cells. Based upon their ultrastructure, association with different parts of gill circulatory system, and cytoplasm density, MRCs have been classified as α and β forms, respectively (Pisam et al., 1987). α-MRCs are concentrated predominantly at the base of the lamella in contact with arterio-arterial circulation whereas β-MRCs are located in the interlamellar regions in contact with arterio-venous circulation. The 'light' cytoplasm of α cells contains more numerous mitochondria and more branched tubular reticulum (TR) bearing Na^+-K^+-ATPase and Ca^{2+}-ATPase than β cells (Wilson and Laurent, 2002). Recently described PNA-positive MRCs that were distinguished from other MRCs by their ability to bind peanut-lectin agglutinin (PNA) and called β cells (Goss et al., 2001; Hawkings et al., 2004), fit the description of α cells defined by Pisam et al. (Pisam et al., 1987). It is still not clear whether α and β cells represent different subtypes of the MRC or different developmental stages in the life cycle of these cells (Wendelaar Bonga and van der Meij, 1989; Perry, 1997).

The most prominent feature of the PVC is the complex pattern of microridges that expand the area of interaction between the cell surface and ambient water. PVC cytoplasm contains few mitochondria, well-developed rough endoplasmic reticulum, and Golgi apparatus that produce microvesicles with an electron-dense core consisting of glycoproteins (Laurent and Perry, 1991; Wilson and Laurent, 2002). When these vesicles fuse with the apical cell membrane, glycoproteins are released to the cell surface and become a component of the glycocalyx or mucous layer. Specialized MCs produce granules of polyanionic mucous containing glycoproteins, mucopolysacharides and carbohydrates (Shephard, 1994). When granules are discharged and burst onto the epithelial surface, their content forms a mucous layer that might be part of the stress response in fish, or may participate in ion and water balance (Shephard, 1994; Wendelaar Bonga, 1997). In a number of teleost fish, the gill epithelium contains rodlet cells (RCs), however, their origin and function remain unknown. They have been proposed to act as non-specific immune cells (Manera and Dezfuli, 2004) or

have a secretory function based upon the presence of rodlet granules rich in glycoproteins and carbohydrates that are released on the epithelial surface (Leino, 1982; Leino, 2001; Matey, 1996).

The scaleless carp (*Gymnocypris przewalskii*) is an endangered species that inhabits Lake Qinghai, a saline (9–13 p.p.t.), alkaline (pH ~9.3) lake on the Qinghai–Tibet plateau at 3200 m. At this altitude, air and water O_2 tensions are about 60% those at sea-level and thus, fish are exposed to chronically reduced O_2 levels (approximately 6 mg O_2 l^{-1}). Mean annual air temperature is –0.6°C, and surface lake water temperatures rarely exceed 13°C in August (Walker et al., 1996). The scaleless carp, however, has an interesting life history relative to most carp species, in that it undergoes an annual spawning migration from the lake into freshwater rivers (Wang et al., 2003; Wood et al., 2006) when they swim 40–50 km over several weeks before reaching their spawning grounds (Walker et al., 1996). Thus, although this species inhabits moderately hypoxic, cool waters, like those of crucian carp or goldfish, it is dependent upon exercise to reach its spawning ground and its body form is superficially more salmonid-like than carp-like.

The objective of this study was to test the hypothesis that gill remodeling during hypoxia is a general characteristic of cold water-dwelling carp, and gill remodeling in hypoxia is associated with an ionoregulatory disturbance. Because the scale-less carp resides in moderate hypoxia (i.e. 3200 m) and has an active lifestyle, the degree of remodeling was expected *a priori* to be reduced relative to that of carp and goldfish (Sollid et al., 2003; Sollid et al., 2005). Special attention was paid to the ultrastructure of filament epithelium cells, such as MRCs, PVCs, MCs and RCs, as in previous studies investigating the effect of hypoxia on gill remodeling, this has not been examined. Fish were collected during their annual spawning migration, allowed to recover for several days, and then exposed to hypoxia (0.3 mg O_2 l^{-1} at 11–15°C) to probe the relative morphological changes of the gills in general, and gill epithelia in particular. Plasma ion levels were measured during exposure to hypoxia to determine the degree to which ionoregulatory status was affected during hypoxia. The scaleless carp is currently listed as endangered, and thus any information that can be gained about its physiology may be important to conservation of this species.

MATERIALS AND METHODS
Fish acquisition and holding

Gymnocypris przewalskii Kessler (approximately 150 g) were collected by beach seine from the Black Horse river, approximately 8 km upstream of the entry point into the South West corner of Lake Qinghai. Fish were collected from 13–26 June, during which time all experiments were conducted, and this time was chosen because it coincided with the annual spawning migration, a time when fish density in the river was high. Fish were transported back to the wet laboratory in aerated buckets and then placed in 160 l plastic tanks, with a density of about 30 fish per tank. Fish were allowed to acclimate for 1–3 days prior to experimentation and were held in flow-through well-water almost identical in composition to the river water, at a temperature of 11–15°C. The wet laboratory was located at the Lake Qinghai Fish Processing Plant (36°33′18″N, 100°38′50″E) on the South Eastern shore of Lake Qinghai and was set up on board a decommissioned fishing vessel supplied with electricity and water that was kindly provided by the management. Fish were collected under permits issued by local and national authorities and all procedures were conducted in accordance with national animal care regulations.

Hypoxia exposure and sampling

The night prior to experiments, 30 fish were transferred to each of two 160 l exposure chambers and left overnight in flow-through, aerated well-water. Hypoxia was achieved by covering the surface of the water with translucent plastic and bubbling the water with nitrogen. Water $[O_2]$ decreased from aerated values of 6 mg l^{-1} (approximately 60% of sea level values at 3200 m but referred to as normoxia throughout this study) to 0.3 mg O_2 l^{-1} (N=10) over the first 1 h of bubbling and then were maintained at 0.3 mg O_2 l^{-1} in both of the chambers for the duration of the hypoxic exposure during which time water O_2 level was continuously monitored using a YSI-85 dissolved oxygen meter (Yellow Springs, OH, USA). Three or four fish were removed from each replicate chamber at 0, 4, 8, 12 and 24 h of hypoxia, or 6 and 12 h after being transferred back to aerated water (N=7 per treatment). Upon removal, fish were immediately euthanized using neutralized MS-222 and terminally sampled. Blood was removed from the caudal vein into a heparinized syringe and plasma was separated and frozen for later ion analysis (at McMaster University, Hamilton, ON, Canada). Plasma Na$^+$, K$^+$, Ca^{2+}, Mg^{2+} were measured using atomic absorption spectrophotometery (AAS; Varian AA 1275, Mississauga, ON, Canada) and plasma Cl$^-$ was measured using the colorimetric mercuric thiocyanate method (Zall et al., 1956). The second gill arch from the right hand side of four fish from each treatment were dissected out, rinsed, and immediately fixed in cold Karnovsky's fixative and transported to San Diego State University, CA, USA (SDSU) for later scanning electron microscopy (SEM), transmission electron microscopy (TEM) and light microscopy (LM) as described below. The second gill arch from the left hand side of the fish was immediately frozen for later measurement of gill caspase 3 activity (commonly used as a biomarker for apoptosis) at Queens University, Kingston, ON, Canada, according to the instruction of the Enzcheck Caspase 3 Assay Kit no. 1 [Z-DEVD-amino-4-methylcumorin (AMC) substrate, cat. no. E13183, Molecular Probes, Invitrogen, Carlsbad, CA, USA] with the following modification. Frozen gill tissue was homogenized in 1× cell lysis buffer (pH 7.5, 1 mmol l^{-1} EDTA, 0.01% Triton X-100). 7-AMC reference standards were made in a 1:1 volume ratio of 1× reaction buffer (pH 7.4, 10 mmol l^{-1} Pipes, 2 mmol l^{-1} EDTA, 0.1% CHAPS) and 1× cell lysis buffer. The caspase 3 activities were assayed by measuring fluorescence (excitation/emission, 342/441 nm) using a 96-well fluoremeter (Molecular Devices, Sunnyvale, CA, USA). The caspase 3 activities were expressed as AMC min^{-1} mg^{-1} protein, where protein content in the homogenate was measured using the bicinchoninic acid (BCA) assay.

Morphological analyses

At SDSU the middle part of each fixed gill arch (≈5 mm long) bearing up to 20 filaments in both anterior and posterior rows was used for scanning electron microscopy. Individual filaments were cut for transmission electron microscopy and light microscopy studies. All fixed gill tissue was rinsed in phosphate-buffered saline (PBS), and post-fixed in 1% osmium tetroxide for 1 h.

Scanning electron microscopy

Gill tissue was dehydrated in ascending concentrations of ethanol from 30% to 100%, critical-point dried with liquid CO_2, mounted on stubs, sputter-coated with gold–palladium, and examined with a Hitachi S 2700 scanning electron microscope at the accelerating voltage of 20 kV.

Transmission electron microscopy and light microscopy

Samples were dehydrated in a graded ethanol–acetone series to 100% acetone and embedded in Epon epoxy resin. Longitudinal semi-thin (1 μm) and ultra-thin (60–70 nm) sections were prepared parallel to the long axis of the filaments and cut with an ultramicrotome (EM-Leica microtome, Bannockburn, IL, USA). Semi-thin sections for LM analyses were mounted on glass slides, stained with 0.5% Methylene Blue and examined in a Nikon Eclipse E200 microscope (Melville, NY, USA). Ultra-thin sections for TEM analyses were mounted on the copper grids, double stained with 2% uranyl acetate, followed by 1% lead citrate, and examined in a Tecnai 12 transmission electron microscope (FEI) at the accelerating voltage of 80 kV.

Morphometry

Various gill parameters were measured in control and experimental fish. These included: (1) protruding lamellar height in contact with ambient water (by LM); (2) lamellar thickness (by LM); (3) protruding lamellar basal length (by SEM); (4) water–blood diffusion distance, from the outer edge of the lamellar epithelium to the inner edge of the endothelium of the lamellar blood vessel (by TEM); (5) thickness of filament epithelium, from the outer edge of the filament to the basal lamina (by LM); (6) number of cell nuclei in the interlamellar space between two neighboring lamellae (by LM); and (7) diameter of apical crypts of MRCs (by SEM). A total of 30 measurements (in ten randomly selected lamellae in three fish, and ten randomly selected filaments in three fish) of each of these parameters was performed in each experimental and control group. The surface area of protruding lamellae (functional respiratory surface) in both control and experimental fish was approximated to a half ellipse and calculated according to the formula proposed by Sollid et al. (Sollid et al., 2003). Three measurements were used for these calculations: (1) basal length of the protruding part of lamellae (l); (2) the height of the protruding part of lamellae (h); (3) the thickness of lamellae (t). The respiratory surface area of lamella was calculated as $a=pl$, where p is the ellipse perimeter formula divided by 2:

$$p = \frac{2\pi \sqrt{\frac{1}{2}(r^2+h^2)}}{2}$$

and $r=t/2$.

Statistical analyses

Morphometric data, gill caspase 3 activity, and plasma [Na$^+$] and [Cl$^-$] levels were expressed as means ±1 s.e.m. and analyzed by one-way ANOVA followed by a *post-hoc* Dunnet's test to identify means that were significantly different ($P<0.05$) from normoxic control values.

RESULTS

Changes in gill morphology

The first alterations in gill morphology were recorded following 8 h exposure to hypoxia. They included a significant decrease in filament epithelium thickness, a reduction in water–blood diffusion distance, and a protrusion of respiratory lamellae and enlargement of their surface area (Figs 1, 2, 3; Table 1). The magnitude of these changes increased following 12 h exposure to hypoxia (Fig. 1B, Fig. 2B; Table 1), where the filament epithelium thickness decreased by about 40% (Fig. 3C), and the surface area of protruding respiratory lamella increased by 50% relative to that of the control (Fig. 3A). By this time, water–blood diffusion

Table 1. Morphometric parameters of the gills, and ionoregulatory status of plasma ion concentrations of the scaleless carp in normoxic and hypoxic water

	Normoxia	Hypoxia				Recovery after hypoxia	
		4 h	8 h	12 h	24 h	6 h	12 h
Gill morphology (μm)							
Protruding lamellar height	78.9±1.7	80.2±1.8	89.1±1.4*	100.6±2.2*	107.2±1.6*	102.3±2.0*	92.4±2.3*
Protruding lamellar basal length	350.8±6.7	356.5±9.0	368.8±9.3*	389.0±10.5*	412.3±11.6*	388.4±7.1*	364.7±8.5*
Lamellar thickness	11.8±0.5	11.8±0.9	10.6±0.6*	9.1±0.3*	8.4±0.4*	10.6±0.8*	11.2±0.4*
Number of nuclei in interlamellar cell mass	17.5±0.6	–	–	12.7±0.5*	10.4±0.2*	10.9±0.4*	12.2±0.3*
Plasma ion levels (mmol l^{-1})							
Ca^{2+}	3.8±0.1	4.0±0.2	3.7±0.2	3.9±0.2	3.6±0.2	3.8±0.2	3.1±0.1*
Mg^{2+}	0.8±0.0	1.2±0.1*	1.0±0.0*	1.0±0.0	0.9±0.0	0.7±0.0	0.8±0.0
K^+	2.1±0.2	2.9±0.2	3.0±0.4	3.9±0.3*	3.4±0.6*	3.4±0.4*	3.2±0.2

Values are means ± s.e.m. *Significantly different ($P<0.05$) from respective normoxic value.

distance decreased by about 40% relative to that of the control (Fig. 3B). Following 24 h exposure to hypoxia, protruding parts of the respiratory lamellae became very thin and long, with a lamellar respiratory surface area approximately 65% greater than that of control fish (Fig. 1C; Fig. 3A). Water–blood diffusion distance and filament epithelium thickness appeared to have reached minimum values (approximately 45% and 50% reductions

relative to controls, respectively; Fig. 3B,C), and in general, gross morphological changes of the gill appeared to be slowing and likely reaching completion (Fig. 3; Table 1). During exposure to hypoxia, only at 24 h was there a significant increase in gill caspase 3 levels (Fig. 4).

Following 6 h recovery, noticeable reversible changes in gill morphology were observed. Filament epithelium thickness was
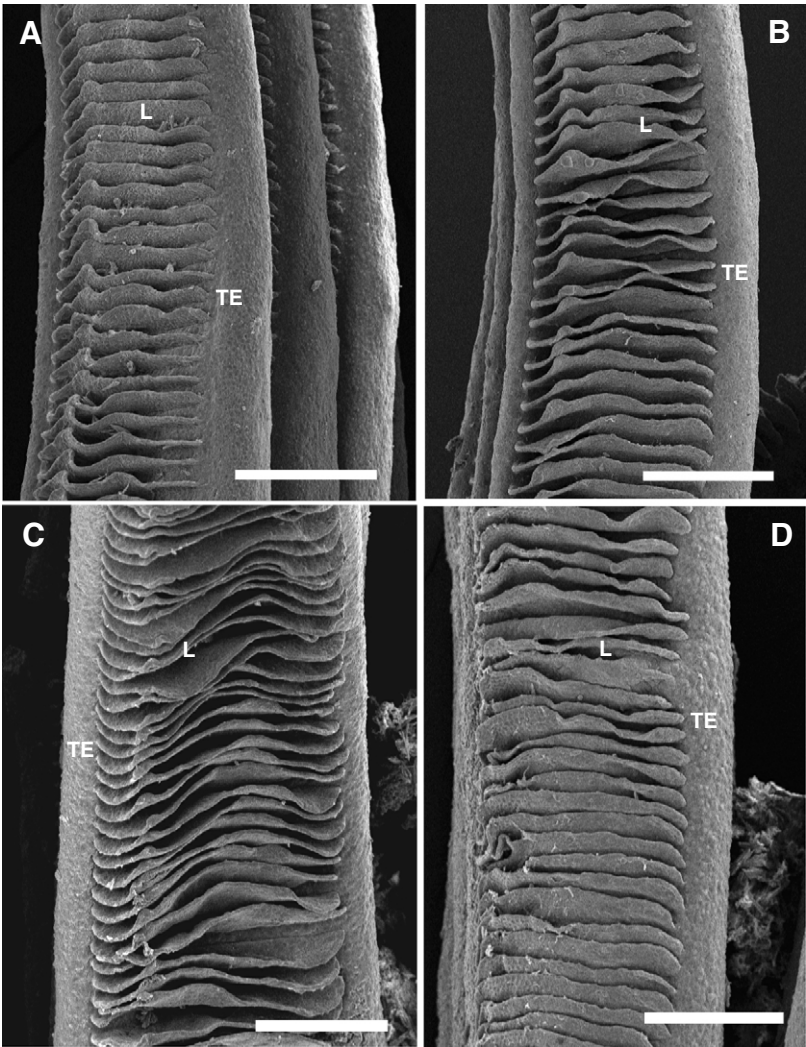

Fig. 1. General view of the scaleless carp gill filaments using scanning electron microscopy (SEM) in fish exposed to normoxia (control; A), following exposure to 0.3 mg O$_2$ l^{-1} hypoxia for 12 h (B), 24 h (C), and following 12 h recovery in normoxia (D). Note that in A, gill filaments bear short lamellae, in B there is an increase in height and basal length of lamellae, which are accentuated in C, and in D there is a reduction in height and basal length of lamellae relative to C. L, lamella; TE, trailing (afferent) edge of filament. Scale bars, 300 μm.
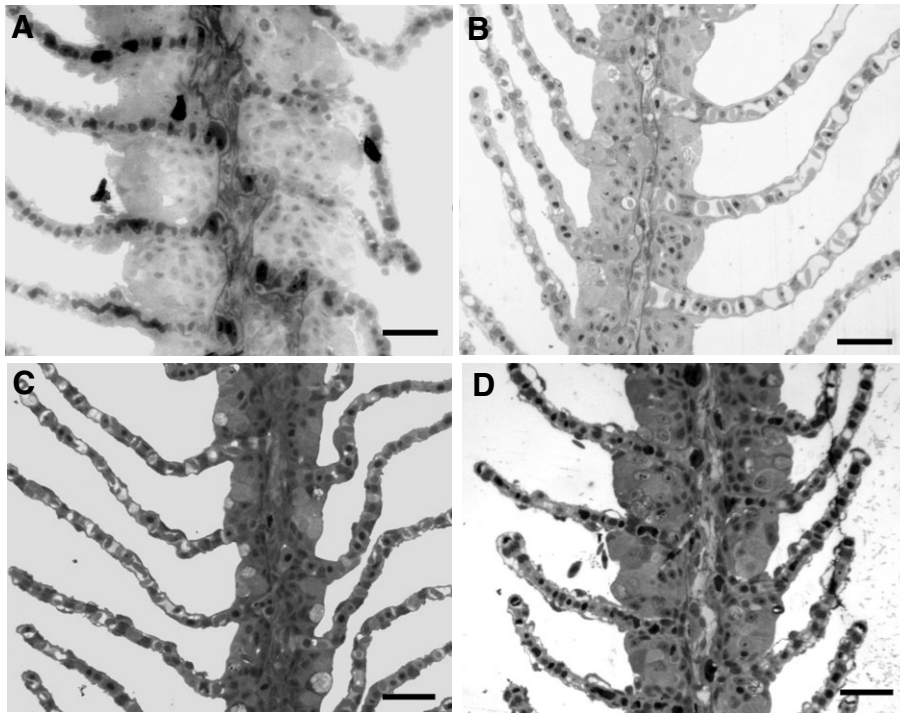
Fig. 2. General view of the scaleless carp gill filaments viewed by light microscopy (LM) in fish exposed to normoxia (control; A), following exposure to 0.3 mg O_2 l^{-1} hypoxia for 12 h (B), 24 h (C), and following 12 h recovery in normoxia (D). Note that in A, the filament is thick and there is an interlamellar mass, in B and C there is a thinning of the filament and lamellar epithelium, and protrusion of the lamellae. In D, there is a thickening of the filament and lamellae, with the reappearance of the interlamellar mass. Scale bars, 20 μm.

slightly increased, resulting in a reduction in protruding lamellar height, length and surface area (Fig. 3A,C; Table 1). While lamellae became thicker, water–blood diffusion distance remained thin (Fig. 3B). The reduction of exposed respiratory lamellar surface area, the thickness of filament epithelium and water–blood diffusion distance approached that of 8 h hypoxia exposed fish (Fig. 1D, Fig. 2D, Fig. 3; Table 1), however, recovery was not complete within 12 h exposure to normoxia.
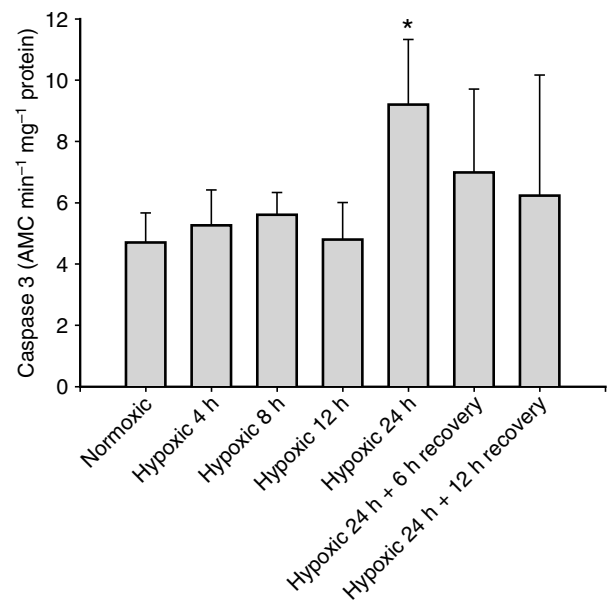

Fig. 3. Changes in (A) protruding lamellar surface area, (B) water–blood diffusion distance, and (C) filament epithelial thickness in the gills of the scaleless carp during exposure to hypoxia (0.3 mg O_2 l^{-1}) for 24 h followed by recovery in normoxia for 12 h. *A statistically significant difference from the normoxic control values. Vertical bars about the mean represent s.e.m. (N=7).

Fig. 4. Caspase 3 activity levels in the gills of scaleless carp during exposure to hypoxia (0.3 mg O_2 l^{-1}) for 24 h followed by recovery in normoxia for 12 h. *A statistically significant difference from the normoxic control values. Vertical bars above the mean represent s.e.m. (N=7).
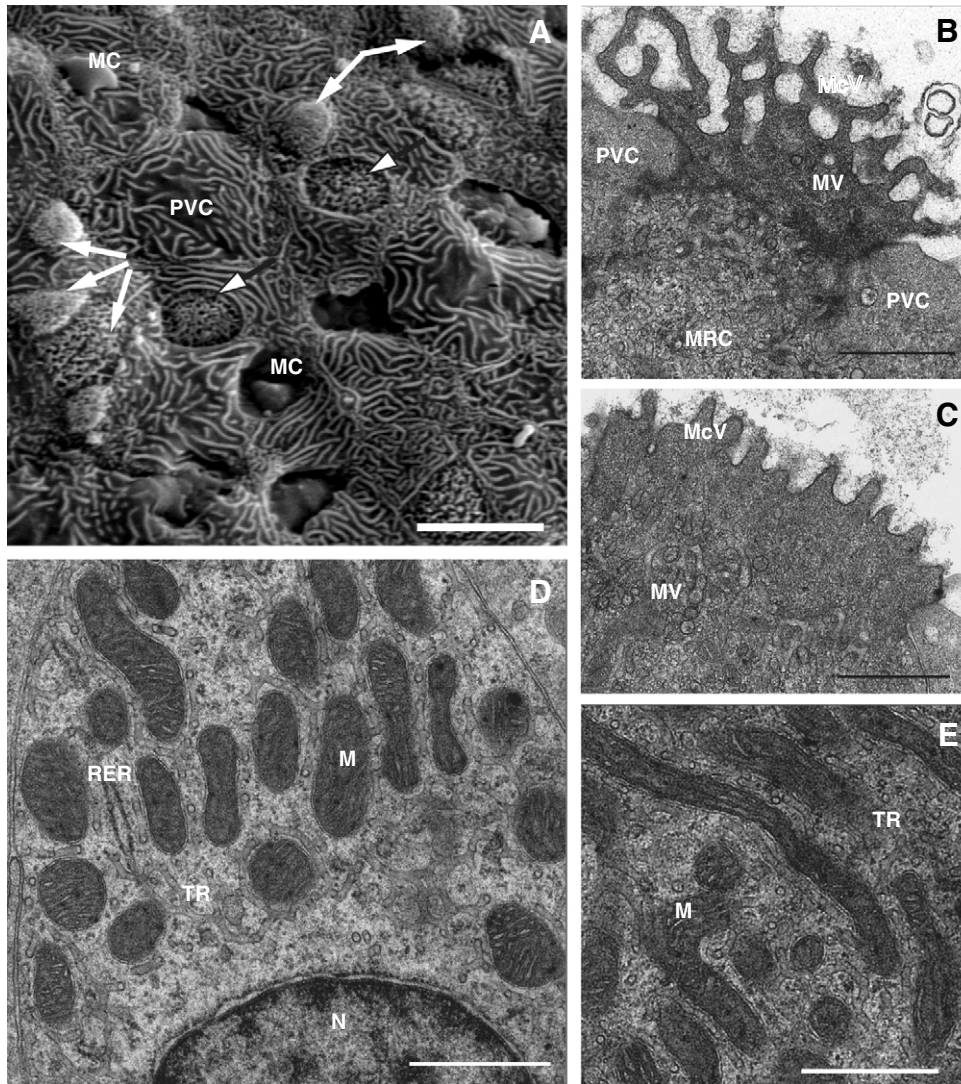
Fig. 5. Ultrastructure of the filament epithelial cells in normoxic control carp viewed by scanning electron microscopy (SEM; A), and transmission electron microscopy (TEM; B–E). A is the surface of the filament epithelium possessing the 'wavy-convex' MRCs with highly ramified microvilli (white arrows) and short and slightly branched microvilli (white-headed arrows), PVCs with complex patterns of microvilli, and a few MCs discharging secretory granules. B is the apical surface of an MRC with highly ramified microvilli, C is the apical surface of an MRC with short microvilli, D is the perinuclear area of an α- ('light') MRC, and E is the perinuclear area of a β- ('dark') MRC. M, mitochondrion; MC, mucous cell; McV, microvilli; MRC, mitochondria-rich cell; MV, microvesicle; N, nucleus; PVC, pavement cell; RER, rough endoplasmic reticulum; TR, tubular reticulum. Scale bars: (A) 10 μm; (B,C) 1 μm; (D,E) 0.5 μm.

Changes in the ultrastructure of gill filament epithelial cells

In control fish exposed to normoxic water, MRCs occurred singly or gathered in clusters in the outer layer of the filament epithelium and consisted only of 'wavy-convex' MRCs (Fig. 5A). Among these wavy-convex MRCs, almost 70% of the cells had broad apical crypts (7.5×5.0 μm) and long and highly branched microvilli, giving the cell surface a net-like appearance under SEM (Fig. 5A,B). About 30% of MRCs had smaller apical crypts (6.8×4.5 μm) and possessed short and less branched microvilli (Fig. 5A,C). Both α- and β-MRCs were present in the filament epithelium of the scaleless carp (Fig. 5D,E). α-MRCs predominated and their apical surface exhibited either long and highly ramified or short and slightly branched microvilli (Fig. 5B,C). The apical surface of β-MRCs possessed only short and slightly branched microvilli.

In PVCs, the apical surface was complex and consisted of long microridges (Fig. 5A). The cell cytoplasm contained numerous microvesicles with an electron-dense filamentous core (Fig. 6A). Fully developed MCs were located in the outermost layer of the filament epithelium and were filled with numerous secretory granules of different electron density (Fig. 6B). There were large pores through which granules can be discharged on the epithelial surface (Fig. 5A). A few developing oval to circular RCs were located in the basal and intermediate layers of the filamental epithelium. They had no access to the epithelial surface but contained rodlet granules in various stages of maturity, with extensively developed rough endoplasmic reticulum and Golgi apparatus (Fig. 6C).

Exposure to hypoxia
Mitochondria rich cells

Following 4 h exposure to hypoxia, noticeable changes were observed in the MRC surface structure (Fig. 7A). Wavy-convex MRCs were present as indicated by cells with enlarged apical crypts (9.1×5.2 μm) bearing short, wide and only slightly branched or unbranched microvilli covered with mucous (Fig. 7A, Fig. 8B). Several α-MRCs were located in the outermost epithelial layer and contained swollen mitochondria, poorly branched tubular reticulum with irregular meshes, and a high density of ribosomes (Fig. 8A). However, the vast majority of α-MRCs did not show any changes in ultrastructure except for an unusually high density of apical microvesicles (Fig. 8B). No changes were observed in the ultrastructure of the less abundant β-MRCs. Following 8 h exposure to hypoxia, MRCs consisted mainly of the α-subtype with smaller
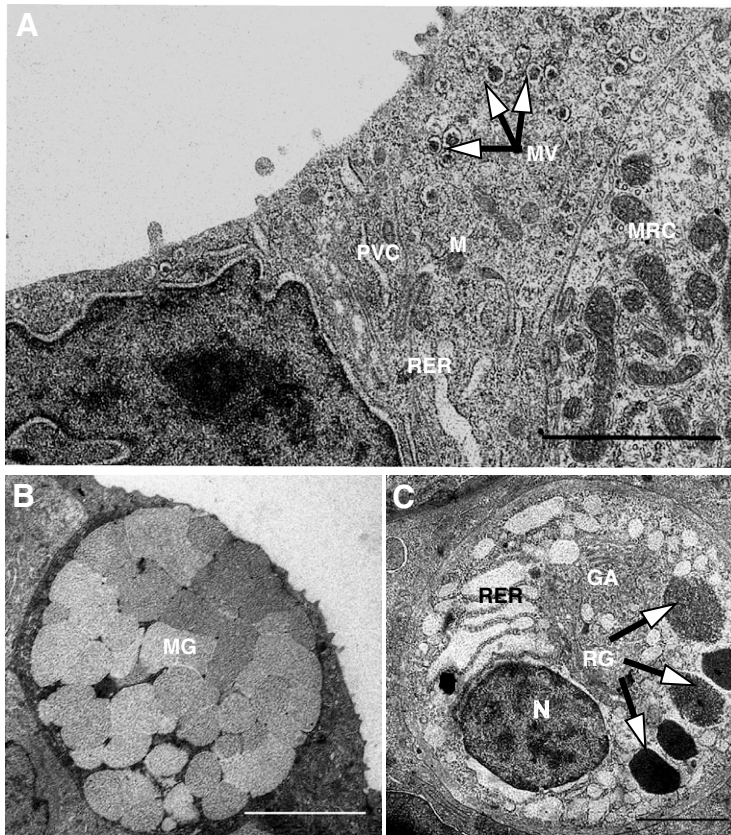
Fig. 6. Ultrastructure of filament epithelium viewed by transmission electron microscopy (TEM) in normoxic control carp. (A) Pavement cell with cytoplasm containing microvesicles with a dense core. (B) Mucous cell filled with secretory granules. (C) Immature rodlet cell with developing rodlet granules. GA, Golgi apparatus; M, mitochondrion; MG, mucous granule; MRC, mitochondria-rich cell; PVC, pavement cell; RER, rough endoplasmic reticulum; RG, rodlet granule. Scale bars, 2 μm.
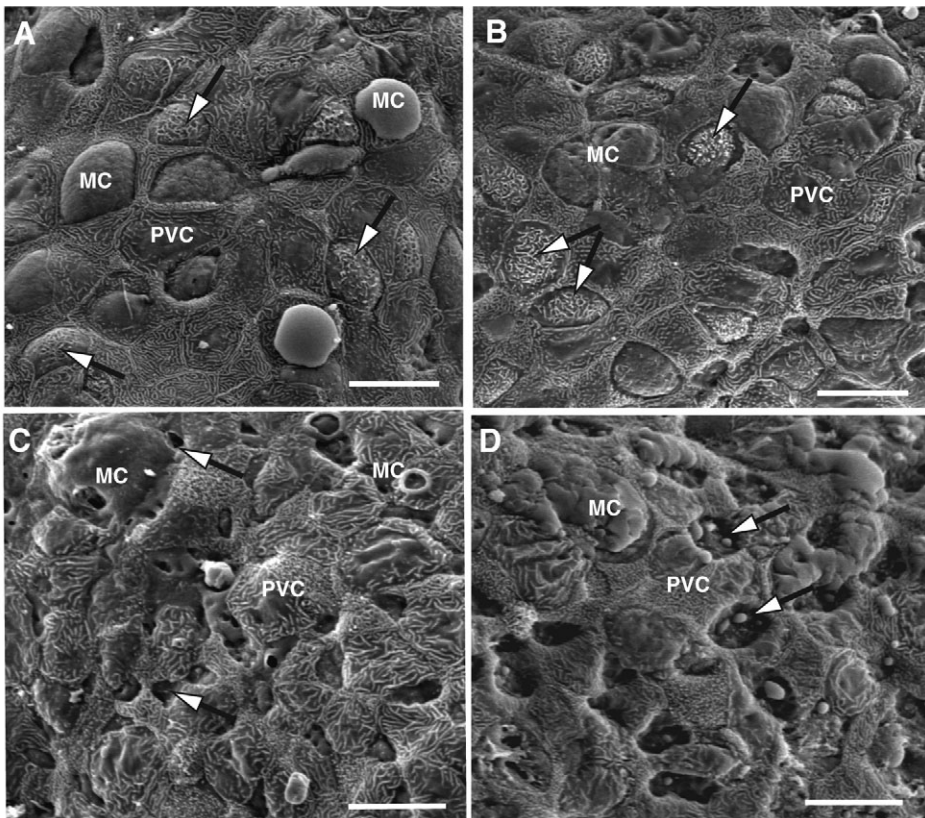

Fig. 7. Ultrastructure of the filament epithelium surface viewed by scanning electron microscopy (SEM) in the scaleless carp exposed to hypoxia (0.3 mg O_2 l^{-1}) for 4 h (A), 8 h (B), 12 h (C) and 24 h (D). In A and B, note the 'wavy-convex' mitochondria-rich cell (MRCs) with short and slightly branched microvilli (arrows) and numerous mucous cells releasing mucous granules; in C, note the small openings of MRCs (arrows), abundant mucous cells, and mucous deposition on the epithelial surface; in D, note 'shallow-basin' MRCs (arrows) with a thick film of mucous covering epithelial surface. Scale bars, 10 μm.

apical crypts (8.7×5.4 μm) and short and 'stumpy' surface microvilli (Fig. 7B, Fig. 8C). Abundant microvesicles were not concentrated exclusively in the apical area but were distributed along the cell up to its perinuclear area (Fig. 8C). No MRCs with altered organelles were observed in the epithelium.

Following 12 h exposure to hypoxia, the epithelial surface exhibited numerous small and deep openings (2.8×1.4 μm) with the appearance of apical crypts of 'deep-hole' MRCs (Fig. 7C). However, TEM revealed that these were not deep-hole but 'shallow-basin' MRCs. They had flat apical surfaces bearing a few short and wide microvilli and were situated below neighboring PVCs on the bottom of the cavities formed with the flanks of PVCs (Fig. 8D). MRCs remained predominantly of the α subtype and contained numerous apical microvesicles located beneath a flattened apical membrane (Fig. 8E). Following 24 h, numerous typical shallow-basin MRCs with large variations in size (from 3.0×2.2 μm to 7.6×3.9 μm) and shape of apical crypts opened directly onto the epithelial surface (Fig. 7D). Few microvesicles were located in the apical area of these MRCs (Fig. 8F). The ultrastructure of both α-MRCs (which still predominated) and β-MRCs did not differ from those in control fish.

Pavement cells

Following 4–8 h of exposure to hypoxia, the surface of most PVCs consisted of shorter, less branched microridges and an expanded microridge-free central area, whereas the remaining PVCs had a surface similar to that of control fish (Fig. 7A,B). At 12–24 h exposure to hypoxia, PVCs displayed a dense array of short microvilli partially or completely masked by mucous (Fig. 7C,D). No alterations were observed in the ultrastructure of PVCs where the cytoplasm was saturated with microvesicles containing an electron-dense core.

Mucous cells and rodlet cells

Following 4 h exposure to hypoxia, MCs appeared to have released mucous that partially masked the convex apical surface and filled apical crypts of the MRCs, complicating identification of MRCs under SEM (Fig. 7B). Patches of thick mucous were deposited on the epithelial surface following 12 h exposure to hypoxia (Fig. 7C). Following 24 h exposure to hypoxia, a thick film of mucous precipitated within the MRC apical cavities, filled spaces between PVCs and covered a large area of the gill filaments (Fig. 7D). TEM indicated groups of two or more MCs filled with secretory granules and numerous RCs at the secretory stage located in the outermost
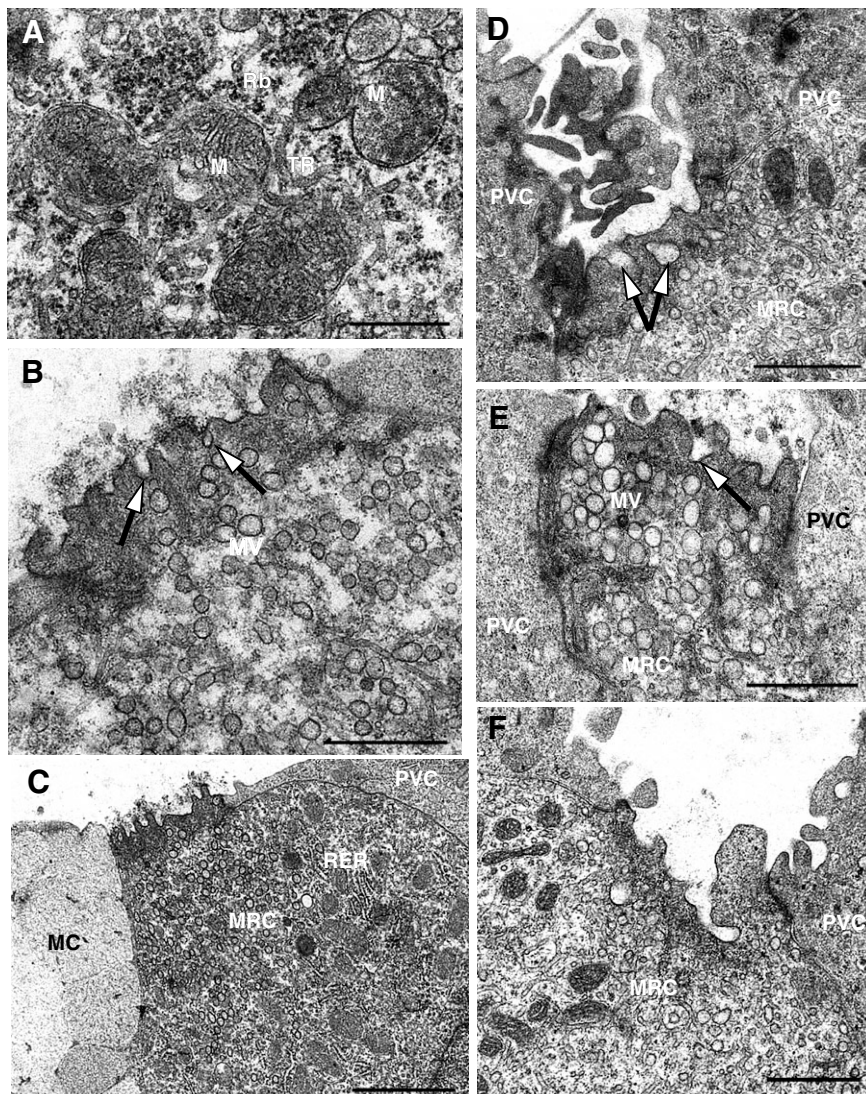

Fig. 8. Ultrastructure of filament epithelial cells viewed by transmission electron microscopy (TEM) in carp exposed to hypoxia (0.3 mg O_2 l^{-1}) for 4 h (A,B) and 8 h (C–F). In A, note the cytoplasm of the α-mitochondria-rich cell (MRC) containing swollen mitochondria, irregular meshes of tubular reticulum (TR) and high concentrations of ribosomes (R). In B note the apical area of the α-MRC with short microvilli, formation of microvesicles (arrows), and the concentration of numerous microvesicles under the apical membrane. In C, note neighboring MRC and mucous cell (MC) and abundant microvesicles spreading from apical to perinuclear area of the MRC. In D, note MRC on the bottom of the cavity formed by flanks of the pavement cells (PVCs). In E, note the MRC with small flattened apical surface and high concentration of microvesicles under the apical membrane. In F, note the cytoplasm of the 'shallow-basin' α-MRC. In B,D,E arrows indicates site of microvesicle (MV) formation. RER, rough endoplasmic reticulum; M, mitochondrion. Scale bars, (A) 0.5 μm; (B,D,E) 2 μm; (C,F) 1 μm.
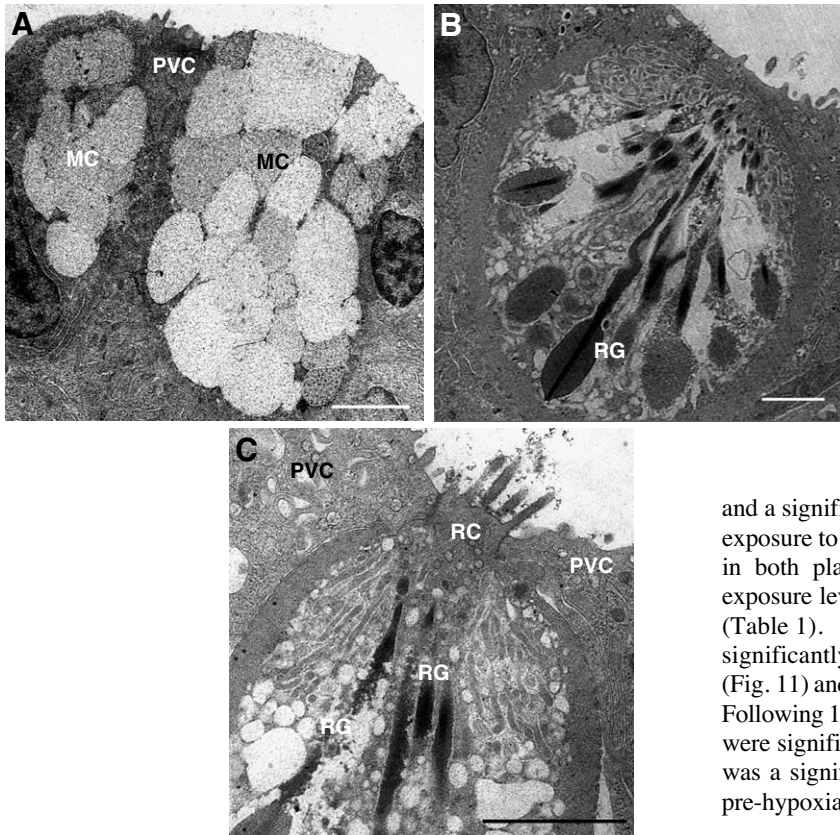
Fig. 9. Ultrastructure of mucous (A) and rodlet (B,C) cells in the outermost layer of the filament epithelium viewed by transmission electron microscopy (TEM) in carp exposed to hypoxia (0.3 mg O_2 l^{-1}) for 24 h. MC, mucous cell; MV, microvesicle; PVC, pavement cell; RC, rodlet cell; RG, rodlet granule; TR, tubular reticulum. Scale bars, (A,B) 2 μm; (C) 1 μm.

epithelial layer which opened directly on to the apical surface (Fig. 9B,C).

Recovery

After 6 h recovery in normoxia, MRCs consisted of a few shallow-basin and numerous wavy-convex forms. The former had slightly concave large apical crypts (6.2×5.5 μm) with few long branched microvilli masked by mucous (Fig. 10A,B). Wavy-convex MRCs with smaller apical crypts (4.4×3.7 μm) possessed short and wide microvilli (Fig. 10A,C). As in hypoxia-exposed fish, shallow-basin MRCs with few apical microvesicles and wavy-convex MRCs without microvesicles consisted mostly of α-MRC (Fig. 10B,C). Following 12 h recovery, shallow-basin MRCs almost disappeared, and wavy-convex MRCs were opened on to the epithelial surface (Fig. 10D–F). Some MRCs had smaller apical crypts (6.9×5.0 μm) and possessed long, highly ramified microvilli, whereas others had larger apical crypts (8.3×5.3 μm) with short and slightly branched microvilli. The epithelial surface was free of mucous that was concentrated only within the crypts of shallow-basin MRCs, similar to that seen following 6 h of recovery. Fewer MCs and solitary RCs were observed in the outermost layers of the filament epithelium. The ultrastructure of PVCs were similar to that following 8 h exposure to hypoxia, exhibiting a simple pattern of short microridges with a microridge-free central zone and abundant microvesicles with an electron-dense core within the cytoplasm (Fig. 10A,D).

Plasma ion levels

Following exposure to hypoxia for 4 and 8 h, there was a statistically significant increase in plasma $[Mg^{2+}]$ (Table 1) relative to pre-hypoxia exposure. Following exposure to hypoxia for 12 h, there was a statistically significant reduction in plasma $[Cl^-]$ (Fig. 11)

and a significant increase in plasma $[K^+]$ (Table 1). Following 24 h exposure to hypoxia there was a significant reduction (by 10–15%) in both plasma $[Na^+]$ and $[Cl^-]$ levels relative to pre-hypoxia exposure levels (Fig. 11) and a significant increase in plasma $[K^+]$ (Table 1). Following 6 h recovery, plasma $[Cl^-]$ remained significantly reduced relative to pre-hypoxia exposure levels (Fig. 11) and plasma $[K^+]$ remained significantly elevated (Table 1). Following 12 h recovery in normoxia, neither plasma $[Na^+]$ nor $[Cl^-]$ were significantly different from control values (Fig. 11), but there was a significant reduction in plasma $[Ca^{2+}]$ (Table 1) relative to pre-hypoxia exposure.

DISCUSSION
General gill morphology and ionoregulatory status during hypoxia

Acute hypoxia altered the general morphology and ultrastructure of the scaleless carp gills. Morphological changes included gradual elongation of the respiratory lamellae, expansion of their respiratory surface area and reduction of water–blood diffusion distance, all of which occurred within 8 to 24 h of exposure to hypoxia (0.3 mg O_2 l^{-1}) and appeared to be tending toward completion by 24 h. The increase in respiratory surface area and reduction in water–blood diffusion distance should facilitate oxygen uptake during hypoxia. The alterations in respiratory lamellae structure were reversible, showing signs of recovery 12 h following return to normoxia. These data are consistent with the results obtained in the crucian carp exposed to long-term hypoxia at a similar temperature (Sollid et al., 2003). The changes occurred more rapidly in the scaleless carp [24 h vs 3–7 days (Sollid et al., 2003)], but the degree of morphological change of the gills was greatly reduced relative to that observed in the crucian carp, which may be a reflection of the more active lifestyle of the scaleless carp, which is known to undertake an annual spawning migration and possesses a more hydrodynamic body form than the crucian carp. It could also be that because the scaleless carp reside in a moderately hypoxic environment (i.e. 60% of sea level water oxygen tensions when in equilibrium with atmospheric O_2 tensions), the extent of the interlamellar mass is reduced relative to that in crucian carp in normoxia at sea level.

The adjustments to hypoxia, which include the morphological changes in the gills, along with possible changes in gill ventilation and perfusion, were associated with up to a 10 and 15% reduction in plasma Na^+ and Cl^- levels, respectively, indicating that these adjustments to secure O_2 uptake have a negative effect on the ionoregulatory status of the fish. Interestingly this was not the case
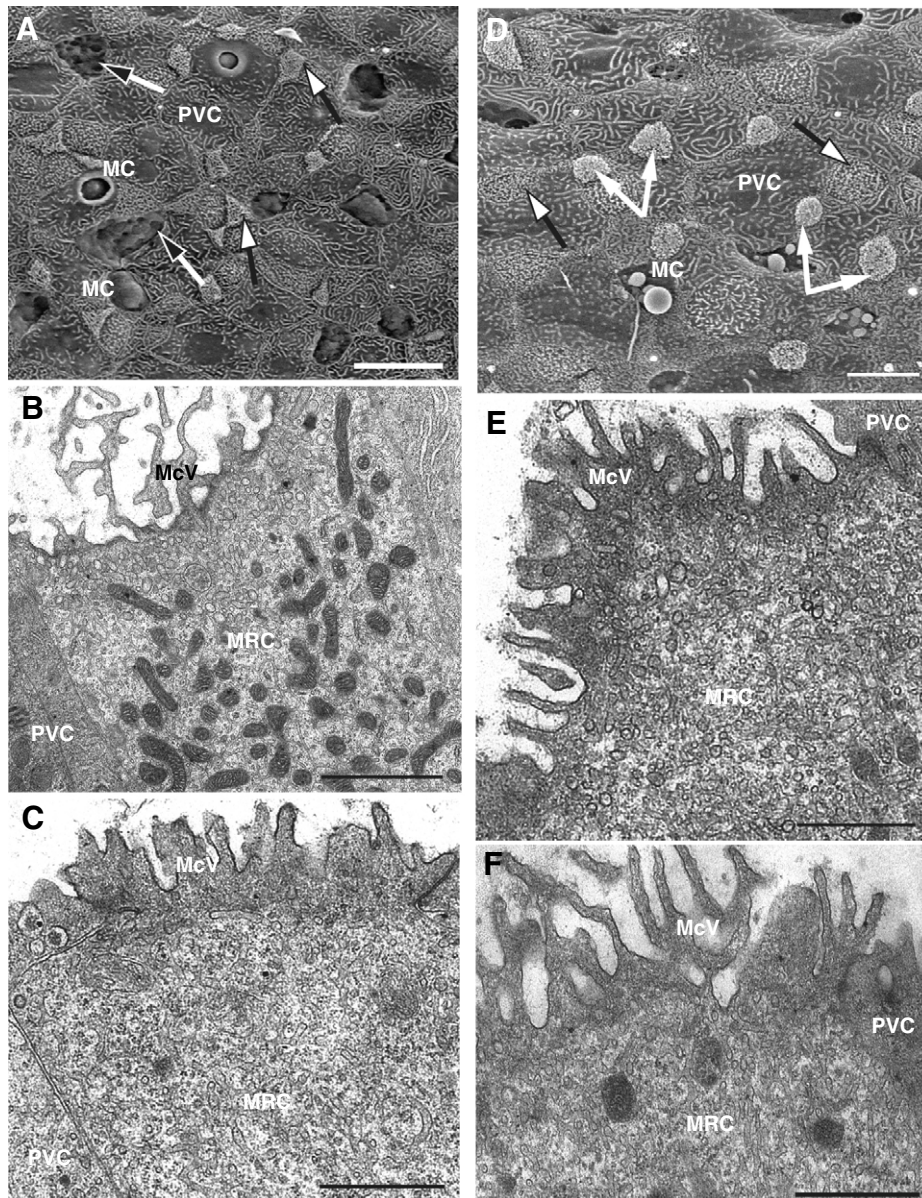
Fig. 10. Ultrastructure of the filament epithelium in carp 6 h (A–C) and 12 h (D–F) following recovery from hypoxia as viewed by scanning electron microscopy (SEM; A,D), and transmission electron microscopy (TEM; B,C,E,F). In A, which shows the epithelial surface, note the mucous cells (MCs), 'shallow-basin' mitochondria-rich cell (MRCs; black-headed arrows) and 'wavy-convex' MRCs with short microvilli (white-headed arrows). In B, note the shallow-basin MRC with branched microvilli protruding from the apical cavity. In C, note the wavy-convex MRC with short, wide, and slightly branched microvilli. In D, which shows the epithelial surface, note the abundant wavy-convex MRCs with branched microvilli (white arrows; McV) and MRCs with short microvilli (white-headed arrows). E and F show the apical area of wavy-convex MRCs with short and strait (E) and branched longer microvilli (F). PVC, pavement cell. Scale bars, (A,D) 10 μm; (B) 2 μm; (C,E,F) 1 μm.

with other ions (Mg^{2+}, Ca^{2+} and K^+), however, these ions occur at much lower concentrations where small changes of 10–15% may not be detectable. There was an increase in plasma [K^+] during hypoxia, which may be indicative of cell damage or muscle depolarization, however, further studies are required to investigate this. The concept of the osmorespiratory compromise was originally developed to describe the trade-off between gas exchange and ionoregulatory requirements during exercise in fish (e.g. Gonzalez and McDonald, 1992). However, the present data illustrate that it applies equally well during hypoxia. Indeed the consequences of the compromise for ionoregulation during hypoxia (approximately 10–15% loss of plasma ions in 24 h) appear to be far greater in the scaleless carp than seen in recent studies on a very hypoxia-tolerant teleost, the Amazonian oscar (Richards et al., 2007; Wood et al., 2007). Thus, although changes in gill morphology during hypoxia probably contribute greatly to hypoxia tolerance in this and other species, the maintenance of this high gill diffusion capacity would probably be a liability to ionoregulation.

The expansion of respiratory lamellae surface area in the scaleless carp is associated with the reduction of filament epithelium thickness due to removal of the interlamellar mass, consistent with the data of Sollid and co-workers (Sollid et al., 2003). Whereas in the crucian carp it is caused by depression of cell proliferation and activation of apoptotic activity of the filament epithelium, in the scaleless carp it may be caused by cell shedding from the outermost epithelial layer. The number of cell nuclei in the interlamellar epithelium decreased by almost 40% after 24 h exposure to hypoxia and became elevated by 30% (relative to 24 h hypoxia) after 12 h of recovery in normoxic water (Table 1). The removal of the interlamellar mass in the scaleless carp may also involve apoptotic pathways as there was a significant elevation in caspase 3 activity (which is commonly used as a biomarker for apoptosis) following 24 h exposure to hypoxia. However, this elevation occurred at a time when most of the morphological changes neared completion and there were no morphological indicators of apoptosis such as nuclear and cytoplasm condensation and distention of mitochondria and components of tubular reticulum (Sardella et al., 2004). In contrast to the cyprinids,
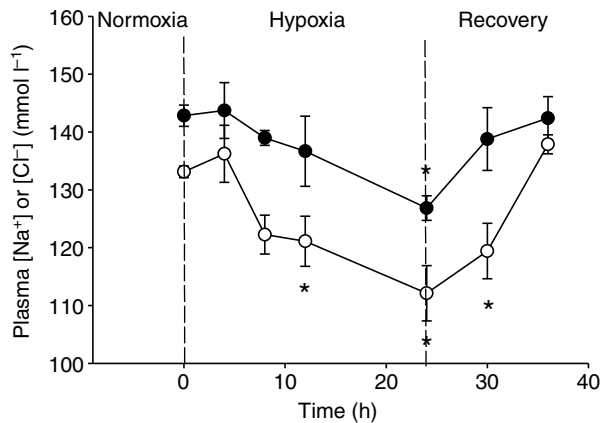
Fig. 11. Changes in plasma [Na$^+$] (filled circles) and [Cl$^-$] (open circles) in the scaleless carp during exposure to hypoxia (0.3 mg O$_2$ l^{-1}) for 24 h followed by recovery in normoxia for 12 h. *A statistically significant difference from the normoxic control values; asterisks below the symbols refer to [Cl$^-$], and that above the symbol refers to [Na$^+$]. Vertical bars about the mean represent s.e.m. ($N=7$).

morphological changes in the gills during exposure to hypoxia have also been seen in the zebrafish, however, the mechanism appears to be different. During hypoxia there is cell proliferation within the respiratory lamellae combined with a reduction in cell size and change in the cell surface, leading to an extension of the lamellar respiratory surface that correlates with changes in gene expression patterns (van der Meer et al., 2005).

Specific changes in filament epithelial cells during hypoxia
Hypoxia clearly induced overproduction and deposition of mucous on the gill surface of exposed fish, which is a generalized response of fish gills to a range of environmental stressors (Mallatt, 1985; Wendelaar Bonga, 1997). Although specialized mucous cells were likely predominantly responsible for the mucous production, other cells may also have contributed. For example, rodlet cells in the secretory stage were observed in close proximity to the mucous cells following 24 h of hypoxia and it is thought that the contents of discharged rodlet granules are mixed with the secretion of MCs becoming a component of gill mucus (Leino, 1982). PVCs possess numerous glycoprotein-containing microvesicles that can fuse to the apical membrane and release their content on the gill surface, and may also have contributed to gill mucous production (Laurent and Perry, 1991). The role of mucous deposition on the gill surface of the scaleless carp during hypoxia is not clear. Although we did not observe the presence of mucous on the lamellar surfaces, the layer of mucous covering gill filaments could be distributed along the gill surface, cover the lamellae, and impair gas diffusion through the respiratory epithelium. However, because of its acidity, polyanionic mucous has been proposed to increase local ion concentrations at the gill surface, facilitate ion exchange and limit water influx (Handy et al., 1980; Shephard, 1994). Thus, mucous may actually reduce the magnitude of the ionoregulatory disturbance associated with the changes in gill morphology noted above, but this clearly requires further investigation.

Acute hypoxia exposure affected MRC morphology, reducing the apical surface area that was exposed to ambient water. In normoxic water, MRCs were exclusively of the wavy-convex type, which have a large surface area and microvilli that may be either long and

branched or short and straight. Exposure to hypoxia led to the disappearance of large MRCs with long and highly branched microvilli. Following 4–8 h of exposure to hypoxia, MRCs with larger apical crypts but few short, wide and slightly branched or stumpy microvilli were opened onto the epithelial surface. TEM revealed a high density of apical microvesicles directly under the apical membrane, indicating that portions of the MRC deeply folded apical membrane were pinched off, forming microvesicles that remained in the apical zone and spread along the MRC cytoplasm. This would limit the extent of the cell surface and resulted in a more smooth appearance. As a result wavy-convex MRCs were transformed into shallow-basin MRCs following 12 h of hypoxia exposure. At this time the shallow-basin MRCs were almost completely covered with neighboring PVCs and had limited access to ambient water. Given that the apical membrane of MRCs is the site for active ion uptake from the water, a reduction in apical surface area may contribute to the progressive reduction in plasma [Na$^+$] and [Cl$^-$] observed during hypoxia.

The alterations in apical morphology of the MRCs were reversible. When fish were returned to normoxic water, MRCs restored their complex surface structure. We hypothesize that this occurred through the fusion of microvesicles (formed from MRC apical membrane removed during hypoxia) with the apical cell membrane. These data indicate that MRCs may regulate their apical surface in response not only to the ionic composition of the water, which has been well documented (Lee et al., 1996; Lee et al., 2000; Chang et al., 2001; Chang et al., 2002; Shieh et al., 2003), but also in response to the oxygen levels of ambient water.

Although hypoxia exposure had a pronounced effect on the apical surface architecture of MRCs, it did not significantly change the internal structure of both the α- and β-type MRCs. Ultrastructure of mitochondria and tubular reticulum and key organelles of MRCs directly linked with ionic regulation appeared similar in control and hypoxia-exposed fish. We hypothesize that the reduction of plasma [Na$^+$] and [Cl$^-$] during exposure to hypoxia is probably a result of the dramatic increase in total gill surface area and the osmorespiratory compromise in conjunction with the reduction in MRC apical surface exposed to the ambient water. Although the former represents a prioritization of gas exchange over ionoregulation during exposure to hypoxia, the basis for the reduction in MRC microvilli during hypoxia is less clear. The large morphological changes in the gill observed in the scaleless carp support the hypothesis that gill remodeling during hypoxia is a general characteristic of cold water carp species and is associated with an ionoregulatory disturbance, however, the reduced magnitude of the response in scaleless carp relative to goldfish and crucian carp may be a reflection of their more active lifestyle or because they reside in a moderately hypoxic environment at altitude.

REFERENCES

Brauner, C. J., Matey, V., Wilson, J. M., Bernier, N. J. and Val, A. L. (2004). Transition in organ function during the evolution of air-breathing; insights from *Arapaima gigas*, an obligate air-breathing teleost from the Amazon. *J. Exp. Biol.* **207**, 1433-1438.

Chang, I. C., Lee, T. H., Yang, C. H., Wei, Y. Y., Chou, F. I. and Hwang, P. P. (2001). Morphology and function of gill mitochondria-rich cells in fish acclimated to different environments. *Physiol. Biochem. Zool.* **74**, 111-119.

Chang, I. C., Lee, T. H., Wu, H. C. and Hwang, P. P. (2002). Effect of environmental Cl⁻ levels on Cl⁻ uptake and mitochondria-rich cell morphology in gills of the stenohaline goldfish, *Carassius auratus. Zool. Stud.* **41**, 236-243.

Evans, D. H., Piermarini, P. M. and Choe, K. P. (2005). The multifunctional fish gills: dominant site for gas exchange, osmoregulation, acid-base regulation, and excretion of nitrogenous waste. *Physiol. Rev.* **85**, 97-177.

Gonzalez, R. J. and McDonald, D. G. (1992). The relationship between oxygen consumption and ion loss in a freshwater fish. *J. Exp. Biol.* **163**, 317-332.

Goss, G. G., Adamia, S. and Galvez, F. (2001). Peanut lectin binds to a subpopulation of mitochondria-rich cells in the rainbow trout epithelium. *Am. J. Physiol.* **281**, R1718-R1725.

Handy, R. D., Eddy, F. B. and Romain, G. (1980). In vitro evidence for the ionoregulatory role of rainbow trout mucus in acid, acid/aluminium and zinc toxicity. *J. Fish Biol.* **35**, 737-747.

Hawkings, G. S., Galvez, F. and Gross, G. G. (2004). Seawater acclimation caused independent alterations in Na⁺/K⁺- and H⁺-ATPase activity in isolated mitochondria-rich cell subtypes of the rainbow trout gill. *J. Exp. Biol.* **207**, 905-914.

Laurent, P. and Perry, S. (1991). Environmental effects on fish gill morphology. *Physiol. Zool.* **64**, 4-25.

Lee, T. H., Hwang, P. P., Lin, H. C. and Hung, F. L. (1996). Mitochondria-rich cells in the branchial epithelium of the teleosts, *Oreochromis mossambicus*, acclimated to various hypotonic environments. *Fish Physiol. Biochem.* **15**, 513-523.

Lee, T. H., Hwang, P. P., Shieh, Y. E. and Lin, C. H. (2000). The relation between "deep-hole" mitochondria-rich cells and salinity adaptation in the euryhaline teleosts, *Oreochromis mossambicus. Fish Physiol. Biochem.* **23**, 133-140.

Leino, R. L. (1982). Rodlet cells in the gill and intestine of *Catostomus commersoni* and *Perca flavescens*: a comparison of their light and electron microscopic cytochemistry with that of mucus and granular cells. *Can. J. Zool.* **60**, 2768-2782.

Leino, R. L. (2001). Formation and release of the secretory product in rodlet cells. Proceedings of the First International Rodlet Cell Workshop. June 14-16, Ferrara, Italy, p 6.

Mallatt, J. (1985). Fish gill structural changes induced by toxicants and other irritants: a statistical review. *Can. J. Fish. Aquat. Sci.* **42**, 630-648.

Manera, M. and Dezfuli, B. S. (2004). Rodlet cells in teleosts: a new insight into their nature and functions. *J. Fish Biol.* **65**, 597-619.

Matey, V. E. (1996). Gills of freshwater teleost fishes: morphofunctional organization, adaptation, and evolution. St. Petersburg: Nauka. [in Russian].

Ong, K. J., Stevens, E. D. and Wright, P. A. (2007). Gill morphology of the mangrove killifish (*Kryptolebias marmoratus*) is plastic and changes in response to terrestrial air exposure. *J. Exp. Biol.* **210**, 1109-1115.

Perry, S. F. (1997). The chloride cell: structure and functions in the gills of freshwater fishes. *Annu. Rev. Physiol.* **59**, 325-347.

Pisam, M., Caroff, A. and Rambourg, A. (1987). Two types of chloride cells in the gill epithelium of freshwater-adapted euryhaline fish, *Lebistes reticulatus*; their modifications during adaptation to seawater. *Am. J. Anat.* **179**, 40-50.

Richards, J. G., Wang, Y. S., Brauner, C. J., Gonzalez, R. J., Patrick, M. L., Schulte, P. M., Choppari-Gomes, A. R., Almeida-Val, V. M. and Val, A. L. (2007). Metabolic and ionoregulatory responses of the Amazonian cichlid, *Astronotus ocellatus*, to severe hypoxia. *J. Comp. Physiol. B* **177**, 361-374.

Sardella, B. A., Matey, V., Cooper, J., Gonzalez, R. J. and Brauner, C. J. (2004). Physiological, biochemical and morphological indicators of osmoregulatory stress in 'California' Mozambique tilapia (*Oreochromis mossambicus × O. urolepis hornorum*) exposed to hypersaline water. *J. Exp. Biol.* **207**, 1399-1413.

Shephard, K. L. (1994). Functions for fish mucus. *Rev. Fish Biol. Fish.* **4**, 401-429.

Shieh, Y. E., Tsai, R. S. and Hwang, P. P. (2003). Morphological modification of mitochondria-rich cells of the opercular epithelium of freshwater tilapia, *Oreochromis mossambicus. Zool. Stud.* **42**, 522-528.

Sollid, J. and Nilsson, G. E. (2006). Plasticity of respiratory structures: adaptive remodeling of fish gills induced by ambient oxygen and temperature. *Respir. Physiol. Neurobiol.* **154**, 241-251.

Sollid, J., De Angelis, P., Gundersen, K. and Nilsson, G. (2003). Hypoxia induced adaptive and reversible gross morphological changes in crucian carp gills. *J. Exp. Biol.* **206**, 3667-3673.

Sollid, J., Weber, R. E. and Nilsson, G. E. (2005). Temperature alters the respiratory surface area of crucian carp *Carassius carassius* and goldfish *Carassius auratus. J. Exp. Biol.* **208**, 1109-1116.

Van der Meer, D. L., van der Thillart, G. E. E. J. M., Witte, F., de Bakker, M. A. G., Besser, J., Richardson, M. K., Spaink, H. P., Leito, J. T. D. and Bagowski, C. P. (2005). Gene expression profiling of the long-term adaptive response to hypoxia in the gills of adult zebrafish. *Am. J. Physiol.* **289**, R1512-R1519.

Walker, K. F., Dunn, I. G., Edwards, D., Petr, T. and Yang, H. Z. (1996). A fishery in a changing lake environment: the naked carp *Gymnocypris przewalskii* (Kessler) (Cyprinidae: Schizothoracinae) in Qinghai Hu, China. *Int. J. Salt Lake Res.* **4**, 169-222.

Wang, Y. S., Gonzalez, R. J., Patrick, M. L., Grosell, M., Zhang, C., Feng, Q., Du, J., Walsh, P. J. and Wood, C. M. (2003). Unusual physiology of scale-less carp, Gymnocypris przewalskii, in Lake Qinghai: a high altitude alkaline saline lake. *Comp. Biochem. Physiol.* **134A**, 409-421.

Wendelaar Bonga, S. (1997). The stress response in fish. *Physiol. Rev.* **77**, 591-625.

Wendelaar Bonga, S. E. and van der Meij, C. J. M. (1989). Degeneration and death, by apoptosis and necrosis, of the pavement and chloride cells in the gills of teleost *Oreochromis mossambicus. Cell Tissue Res.* **255**, 235-243.

Wilson, J. M. and Laurent, P. (2002). Fish gill morphology: inside out. *J. Exp. Zool.* **293**, 192-213.

Wood, C. M., Du, J., Rogers, J., Brauner, C. J., Richards, J. G., Semple, J. W., Murray, B. W., Chen, X-Q and Wang, Y. (2006). Przewalski's naked carp (*Gymnocyypris przewalski*): an endangered species taking a metabolic holiday in Lake Qinghai, China. *Physiol. Biochem. Zool.* **80**, 59-77.

Wood, C. M., Kajimura, K., Sloman, K. A., Scott, G. R., Almeida-Val, F. F. and Val, A. L. (2007). Rapid regulation of Na⁺ fluxes and ammonia excretion in response to severe hypoxia in the amazonian oscar, *Astronotus ocellatus. Am. J. Physiol.* **292**, R2048-R2058.

Zall, D. M., Fisher, D. and Garner, M. D. (1956). Photometric determination of chlorides in water. *Anal. Chem.* **28**, 1665-1678.